PHYSICAL REVIEW B VOLUME 26, NUMBER 10 15 NOVEMBER 1982

Growth of spontaneous periodic surface structures on solids during laser illumination

Zhou Guosheng,* P. M. Fauchet, and A. E. Siegman
Edward L. Ginzton Laboratory, Stanford University, Stanford, California 94305
(Received 28 June 1982)

Spontaneous periodic surface structures, or ripples, are frequently observed after illumination of metals, semiconductors, and dielectrics by intense laser pulses. We develop a theory which predicts the observed spacing, polarization, and growth properties of these ripples. In this model, one or several Fourier components of a random surface disturbance scatter light from the incident beam very nearly along the surface. The interference of this diffracted optical wave with the incident beam then gives rise to optical interference fringes which can reinforce the initial disturbance. Sinusoidal corrugations on either metallic or molten surfaces seem to provide strong positive feedback for ripple growth, whereas sinusoidal gratings in temperature, electron-hole density, or dielectric constant seem much less well correlated with observations.

I. INTRODUCTION

With the advent of moderate- to high-power laser sources it has become possible to easily transform the properties and structure of many solids with the use of laser radiation. Some of these laser-induced phase transformations are useful and can be produced intentionally, as in laser-induced welding and hardening,[1,2] and laser annealing.[2–4] In other cases the transformations are unwanted and must be avoided, as with laser-induced damage.[5] However, most of these phenomena have in common the fact that the laser source strongly excites the solid and brings it to a state far from equilibrium. Examples of such excitation include boiling, melting, and the creation of a large density of free carriers.

Recently, there have been several reports on a phenomenon frequently observed during illumination of solids by intense laser pulses, namely, the appearance of spontaneous periodic surface structures, or ripples, with spatial periods closely related to the optical wavelength. These ripples have been produced in metals, semiconductors, and dielectrics, by lasers operating at wavelengths from the middle infrared to the blue end of the visible spectrum, and having pulse lengths ranging from cw operation to picosecond pulses.

In this paper we investigate in some detail a family of mechanisms capable of triggering the formation of such periodic ripples. Owing to the wide variety of experimental conditions under which these ripples have been produced, it is difficult to assert that one unique mechanism is at work. We will therefore restrict ourselves to studying the most commonly observed type of surface topography, described in Sec. II of this paper. Although we do not claim that our model and its conclusions are universal, we have tried to keep our theory as general as possible.

The paper is organized as follows. In Sec. II we review the experimental evidence and the mechanisms suggested by others. Our model is outlined in Sec. III. In Sec. IV it is applied to two important cases: a corrugated surface and a periodic dielectric function. Finally, in Sec. V, the results of Sec. IV are discussed and the possible feedback mechanisms for ripple growth are investigated.

II. EXPERIMENTAL RESULTS AND PREVIOUS MODELS

A. Experimental observations

In this section most of the experimental evidence accumulated since 1973 concerning surface ripples is reviewed. Figure 1 shows ripples obtained by us after picosecond laser illumination of GaAs. Table I shows in which materials and at which wavelengths surface ripples have been observed. In this list we do not include surface undulations caused by edge effects[22] or by scattering from dust particles.[23] The resulting surface topography in these cases, although somewhat reminiscent of the periodic surface structure of interest in this paper, is clearly caused by readily understood scattering phenomena,

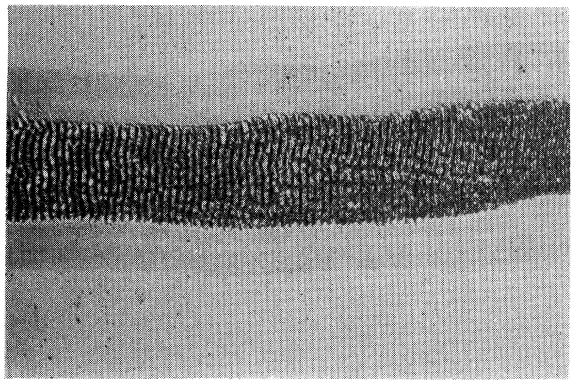

FIG. 1. Typical ripples obtained after raster scanning of GaAs at 1.06 μm. The angle of incidence is $\sim 37°$ and the spacing is ~ 2.5 μm.

and indeed, does have properties quite different from those listed below.

As can be seen from Table I the ripples of interest here have been produced in metals (Al,Cu,Ni_xP_{1-x}), in semiconductors (Si,Ge,GaAs), and in dielectrics (fused silica, quartz, glass). Since, to our knowledge, no systematic search for other materials has been done so far, we are inclined to believe that many other materials will exhibit similar surface structures at many different wavelengths.

In the earliest reports surface ripples were obtained after illumination at 10.6 μm on Cu, Ni_xP_{1-x}, Ge, and various dielectrics. The pulse duration in those experiments was submicrosecond, and the peak power varied from 100 MW/cm^2 to 10 GW/cm^2. In all the other experiments, performed in the visible or near infrared, the laser pulse was either in the nanosecond regime (Q-switched lasers) or in the picosecond regime (mode-locked lasers). The only exception is in Ref. 13 where a cw argon ion laser produced ripples on ion-implanted silicon. For Q-switched lasers the pulse duration varied from less than 10 to more than 100 ns and the peak power was in the range of 100 MW/cm^2. For mode-locked lasers the pulse duration was ≤ 100 ps and the peak power exceeded 1 GW/cm^2. In all cases the actual numbers depend upon the material, its structural form (ion implanted, polycrystalline, or single crystal), its surface quality, and the wavelength of the laser. The surface ripples produced under these widely different conditions have, nevertheless, a large number of properties in common, which we review now.

1. Spacing and polarization

The crests and valleys of the ripples are almost always found to run perpendicular to the incident electric field (i.e., grating k vector for the ripples parallel to the E field vector). At normal incidence the ripple spacing Λ in nearly all cases is approximately equal to the wavelength in vacuum λ. There are, however, a few exceptions.[12,18,19] For oblique incidence and TM or p polarization (i.e., the incident electric field is in the plane of incidence) the ripples occur with one or the other of two spacings Λ given by

$$\Lambda = \frac{\lambda}{1 \pm \sin\theta} , \tag{1}$$

where θ is the angle of incidence measured from the normal to the surface. The occurrence of these two spacings is irregular, and the factors determining which spacing will occur have not been determined.

TABLE I. References in which periodic surface structures such as the ones examined here have been reported. Each reference is listed at the end of the paper and we have indicated in which materials and at which wavelengths the surface ripples have been observed.

	Wavelength (μm)				
Material	~ 10	1.06	0.69	0.53	~ 0.5
Al		16,20			
Cu	6	21			
Ni_xP_{1-x}	10				
Brass		20			
Si		11,14,15,17,18	18	15,17,18	13
Ge	6,7,8,9	20			
GaAs		17	12	17	
Fused silica quartz	8,19				
Glass	6				

Ripples with both of these spacings are sometimes found intermingled in the same area. For oblique incidence with TE or *s* polarization the spacing remains equal to the wavelength. For circular polarization no ripples are observed.

We note that in a few instances a somewhat richer structure, with topographical features running both perpendicular and parallel to the incident electric field, has been reported.[9,15,17,19,21] Since the properties of the "parallel" structures vary widely from author to author, we will not include them here.

2. *Growth and propagation*

Ripples can be produced by a single laser shot or by many laser shots. Optical pulses with intensities substantially less than that required for single-shot ripple formation can still produce ripples after many shots so that the threshold for formation of ripples by successive illumination apparently decreases significantly with an increasing number of shots.[15,17,19] It is also possible to observe the growth of the periodic structure from shot to shot, until the whole spot is filled with ripples and eventually becomes badly damaged.[15,19,21]

If the laser beam is moved between shots such that two successive spots still partially overlap, two possibilities occur.[17,21] If the displacement is parallel to the incident electric field the ripples can extend coherently over many laser shots, but for displacements perpendicular to the incident electric field the ripples in one spot have, in general, no phase relationship with the ripples in an adjoining spot.

3. *Other properties*

Ripples appear to be produced independently of the atmosphere in contact with the solid surface. The only exception is Ref. 10, in which it was found that oxygen had to be present in the atmosphere for the ripples to be produced. We have also recently found that for semiconductor surfaces in contact with a fluid of index of refraction n, the ripple spacing Λ scales as $1/n$.[21] In crystalline media the properties of the ripples are also independent of the crystallographic orientation. Finally, in many experiments the ripples appear most strongly at intensities close to the melting threshold.[11–13,16,17] For example, Fig. 1 in Ref. 17 shows the result of 80-ps pulse laser annealing of ion-implanted silicon at 532 nm. The center of the spot has been transformed into single crystal, while the outer annual region is made of fine-grain polycrystalline material. Surface ripples appear in an annular ring between these two regions. Although the true mechanism of pulsed laser annealing is still somewhat controversial,[24–26] the prevalent opinion is that amorphous to single-crystal transitions are accompanied by melting.[27–29] We shall come back to that problem, and to the more general problem of highly excited solids, when we discuss the implications of our model.

B. Proposed mechanisms

We now turn our attention to the various mechanisms suggested to explain the experimental evidence. Emmony *et al.*[7] first suggested that a scattering center on the surface might be responsible for the observed ripples. The interference of an incident wave with waves scattered by a dust particle or scratch, will produce intensity fringes with a spacing equal to the laser wavelength under normal incidence. By illuminating tilted samples having appropriate scratches they also experimentally verified Eq. (1).

Leamy *et al.*[11] later expanded this idea by suggesting that, as a consequence of these intensity fringes, the melting threshold was periodically exceeded, leaving alternating regions of different crystallinity. The main requirement is that the average temperature of the surface be close to the melting temperature.

Willis and Emmony[9] later explained their observations on germanium samples, in terms of the appearance of electron avalanches around low ionization energy centers, close to or at the surface. A radiating doublet might thus be formed at the interface between the two media, and it therefore becomes easier to produce another doublet where the laser radiation and the emission from the initial doublet interfere constructively. This could result in an array of doublets, all radiating in phase. According to Becker, Walser, and co-workers,[15,30] who have modified this idea and adapted it to the case of silicon, the mechanism is resonant absorption of photons by plasmons at the surface of small metallic spheres, or droplets, of a critical size. The droplets would be produced by thermal fluctuations driving the excited solid locally above melting temperature. A requirement is that the solid under excitation be close to a chemical instability.

Maracas *et al.*[12] argued that there is a standing

acoustic wave pattern corresponding to the axial-mode beat frequencies of their ruby laser, resulting in a periodic melting of their GaAs samples. Their ripple spacing was $\sim 6.5\lambda$, while the experiments of all the others indicate a ripple spacing much closer to λ, if not equal to it, for normal incidence illumination.

Finally, several authors have suggested that surface plasmons or surface polaritons could produce the ripples. Van Vechten[31] first proposed that ripples may occur as a consequence of the condensation of plasmons in very high carrier-density regions. This suggestion was made in the context of the nonthermal or plasma model of pulsed laser annealing. Rendell and Ngai[32] put forth qualitatively similar ideas. Keilmann and Bai,[19] working in the infrared reststrahlen region of quartz, produced some evidence for a dispersive behavior of the ripple period, and attributed that phenomenon to the action of surface polaritons.

In the following section we outline our own model, in which we have tried to refine and generalize some of the above ideas. In Sec. IV we apply it by carrying on a detailed theoretical analysis of two interesting cases. Section V will discuss the impact of several factors, such as pulse length or intensity, and will present a comparison between our results and those of the other models.

III. MODEL

The most striking and clearcut aspect of the experimental evidence seems to be the wavelength and angle dependence of the ripple spacing given by Eq. (1). Figure 2 shows, for example, our results[17] for the ripple spacing versus the angle of incidence θ, in the case of p-polarized, $\lambda = 1.06$ μm pulses on Si and GaAs. Given this angular dependence it seems obvious that the surface ripples must be produced by interference of the incident laser beam with an optical wave travelling very nearly along the surface with a velocity equal to, or very close to, the velocity of light in free space. The upper branch ($\Lambda > \lambda$) then comes from the interference of the incident beam with the downward-travelling surface wave, while the lower branch ($\Lambda < \lambda$) comes from interference with the upward-travelling wave. For normal incidence the scattered wave can travel in either direction, or in both at once, giving $\Lambda \equiv \lambda$. Our observation that the ripple period can be scaled as $1/n$ by immersing the surface in a liquid of index of refraction n particularly reinforces these conclusions.

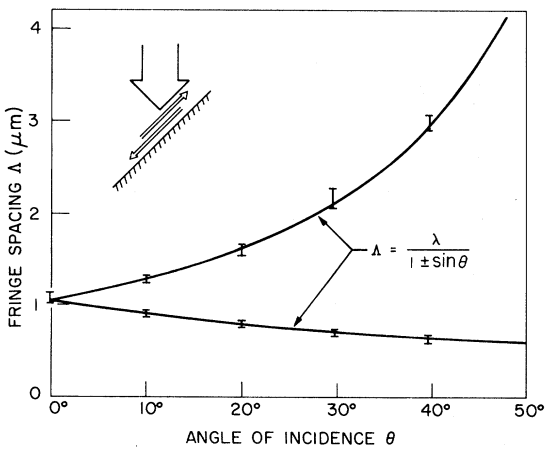

FIG. 2. Ripple spacing Λ vs angle of incidence θ for p-polarized, $\lambda = 1.06$ μm pulses on Si and GaAs.

At this stage, we need to answer two questions: (1) What is the reason for the existence of an optical wave travelling along the surface, and (2) is the complete mechanism self-reinforcing or, in other words, will feedback and exponential growth occur? To answer the first question, we note that a real sample surface will have a finite surface roughness, corresponding to random surface disturbances in height. The surface of an absorbing solid under laser-light illumination may also be characterized by a nonuniform temperature and/or electron density. These random variations may be caused by the height variation itself, by the poor crystalline quality of the surface layer, or by any other intrinsic or extrinsic cause.

These random surface disturbances can then be viewed as the superposition of many different surface gratings with different spatial periods Λ_i. Consider, in particular, any one of these surface grating components with an arbitrary spatial frequency or spatial period given by Λ_i. This periodic surface component will then diffract light from the incident beam into a number of diffracted orders at angles given by standard diffraction theory; the light scattered into these orders will then interfere with the originally incident wave to produce an intensity pattern on the surface which has the same period Λ_i as the original grating component (or else an integer multiple of this).

Any period Λ_i of the initially random surface grating can thus produce an interference pattern on the surface which may cause optically induced growth of that grating component. Those periodic grating components with periods given by Eq. (1), however, will diffract light from the incident beam along the surface, either upward or downward, as il-

lustrated in Fig. 1; one might expect that scattered light coming from these grating periods and travelling along the surface should interact "longest and strongest" with the material surface itself.

At this stage we must thus consider the second question, i.e., will this optical interference lead to the growth of the initial grating disturbance with spacing Λ? This question is illustrated in the flowchart of Fig. 3. To appreciate the importance of this point let us consider an example taken from Sec. IV and schematically illustrated by Fig. 4. We assume an initial sinusoidal temperature disturbance of period Λ at a surface illuminated under normal incidence. Since the index of refraction of such a surface is temperature dependent, it will also follow a similar periodic variation. The index variation then acts like a grating,[33] and the light intensity, and therefore the power absorbed, also becomes modulated with the same period. The phase of this modulation, however, may or may not reinforce the initial temperature disturbance. Figure 4 illustrates the two extreme cases. If the power absorbed is given by the solid line, we see that regions that are already warmer will experience a faster rate of temperature increase, and the temperature difference between the shaded and nonshaded regions will increase. As a result the index variation also increases, the diffraction is stronger, and the intensity fringes are more pronounced. Positive feedback is established and growth occurs. On the other hand, if the power absorbed is given by the dashed line, more power will flow into regions that were initially colder and any initial perturbation will soon be erased, resulting in a no-growth situation.

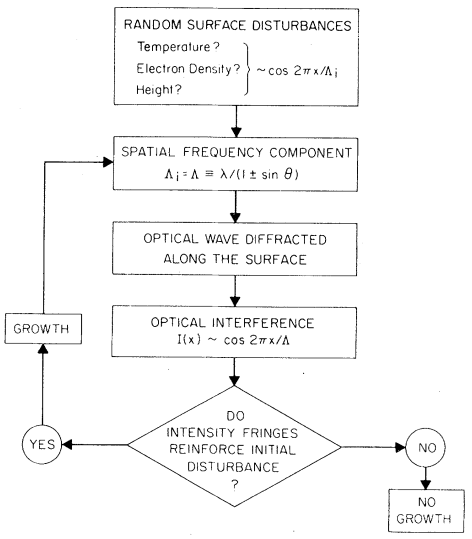

FIG. 3. Flowchart illustrating our model for ripple growth.

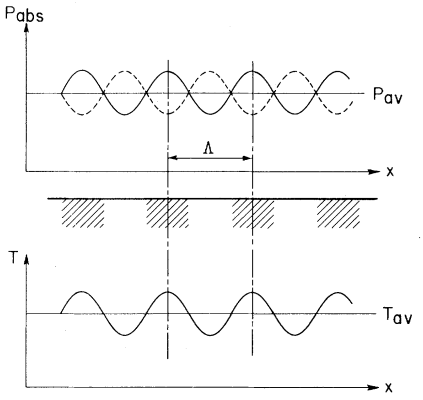

FIG. 4. Schematic illustration of positive and negative feedback for a sinusoidal variation of the temperature. (The dashed regions correspond to $T > T_{av}$). The absorbed power is either in phase (solid line) or out of phase (broken line) corresponding to positive and negative feedback, respectively.

The exponential growth resulting from positive feedback in this case is analogous to periodic small-scale self-focusing in dielectrics.[34,35] As suggested by Bespalov and Talanov in 1966, and demonstrated experimentally by Campillo *et al.* in 1973, small-scale self-focusing can be viewed as an instability phenomenon in which any initial perturbation (for example, in the index of refraction) may grow to catastrophic proportions, provided it corresponds to a situation associated with a positive growth rate. If that is the case, the initial perturbation may be arbitrarily small, and for a random initial perturbation, the component(s) with the largest growth rate will dominate.

In our problem the situation is clearly similar. Only one (or two for oblique incidence) Fourier component should grow, with the others corresponding either to lower or negative growth rates. By comparing the sign and magnitude of the growth rate for three possible initial surface disturbances we will be able to predict the most likely mechanism for ripple formation for each solid.

Finally, our model has to be consistent with all the experimental facts. The spacing and polarization properties, in particular, have to be recovered. In Sec. IV we consider in some detail the two cases of interest: a corrugated surface (height disturbance) and a variation of the dielectric function (temperature or electron density disturbance).

IV. CALCULATIONS

A. Corrugated surface

Consider the situation of a small sinusoidal surface corrugation as illustrated in Fig. 5. The corrugated vacuum-solid interface is described by the following surface equation:

$$z(x)=-h\cos\frac{2\pi}{\Lambda}x\ , \tag{2}$$

where Λ and h are the spatial period and the amplitude of the corrugation, respectively. The z axis is the outward normal to the macroscopic surface, and the x axis is perpendicular to the ripples. A plane wave is incident on the surface, with an angle of incidence θ_i. Scattering from such a sinusoidal interface has recently been summarized in some detail by Chuang and Kong.[36] We shall use their general analysis to derive results that are relevant to our problem, namely, the surface phenomena, which they did not consider specifically.

The fields in the vacuum ψ_0 and in the medium ψ_1 are described through Maxwell's equations by

$$\nabla^2\psi_0+k^2\psi_0=0\ , \tag{3}$$

$$\nabla^2\psi_1+K^2\psi_1=0\ . \tag{4}$$

The electric field $\vec{E}_{0,1}$ is then expressed by $\vec{E}_{0,1}=\psi_{0,1}\hat{y}$ for a TE wave, and the magnetic field by $\vec{H}_{0,1}=\psi_{0,1}\hat{y}$ for a TM wave, where $\hat{y}$ is the unit vector in the y direction. The wave number in the vacuum and in the medium are, respectively, given by $k=\omega\sqrt{\mu_0\epsilon_0}$ and $K=\omega\sqrt{\mu_0\epsilon_1}$, where μ_0 is the magnetic permeability, and ϵ_0 and ϵ_1 are the dielectric constant (permittivity) of the vacuum and the medium, respectively. In general, ϵ_1 is a complex number. The reflected and refracted waves follow the grating equations

$$k\sin\theta_n=k\sin\theta_i+n\frac{2\pi}{\Lambda}\ , \tag{5}$$

$$K\sin\phi_n=k\sin\theta_i+n\frac{2\pi}{\Lambda}\ , \tag{6}$$

where n is an integer, and θ_n and ϕ_n are the angles of the nth-order reflected and refracted waves, respectively. Following the notation of Ref. 36 we let $\alpha_n=\sin\theta_n$ and $\alpha_n'=\sin\phi_n$, and we rewrite Eqs. (5) and (6) as

$$\alpha_n=\sin\theta_i+n\frac{2\pi}{\Lambda}\frac{1}{k}\ , \tag{7a}$$

$$\alpha_n'=\frac{k}{K}\sin\theta_i+n\frac{2\pi}{\Lambda}\frac{1}{K}\ , \tag{7b}$$

$$k\alpha_n=K\alpha_n'\ . \tag{7c}$$

We also define two useful quantities, β_n and β_n', as

$$\beta_n=\begin{cases}(1-\alpha_n^2)^{1/2} & \text{for } \alpha_n^2\le 1\\ i(\alpha_n^2-1)^{1/2} & \text{for } \alpha_n^2>1\ ,\end{cases} \tag{8}$$

$$\beta_n'=\begin{cases}(1-\alpha_n'^2)^{1/2} & \text{for } \alpha_n'^2\le 1\\ i(\alpha_n'^2-1)^{1/2} & \text{for } \alpha_n'^2>1\ .\end{cases} \tag{9}$$

We now wish to consider specifically the situation of interest to us in order to simplify the formalism of Ref. 36. We are dealing with cases in which the first-order reflected wave travels in the direction of, or close to, the x axis. Equation (1) should therefore hold, at least approximately. In Fig. 6 we present a k-vector diagram for a wave incident at θ_i. By requiring that the first-order scattered waves lie along the x axis ($\vec{k}_{\pm1}||\hat{k}_x$) we indeed find the two spacings of Eq. (1).

By keeping only the first-order diffracted waves one obtains[36] for the incident waves

$$\psi_i(\vec{r})=\frac{1}{\sqrt{\beta_0}}e^{i(k\alpha_0x-k\beta_0z)}\ , \tag{10}$$

for the reflected waves

$$\psi_0(\vec{r})-\psi_i(\vec{r})=\sum_{n=-1}^{1}\frac{b_n}{\sqrt{\beta_n}}e^{i(k\alpha_nx+k\beta_nz)}\ , \tag{11}$$

and for the refracted waves

$$\psi_1(\vec{r})=\sum_{n=-1}^{1}\frac{A_n}{\sqrt{\beta_n'}}e^{i(K\alpha_n'x-K\beta_n'z)}\ , \tag{12}$$

where the coefficients A_n and b_n have been calculat-

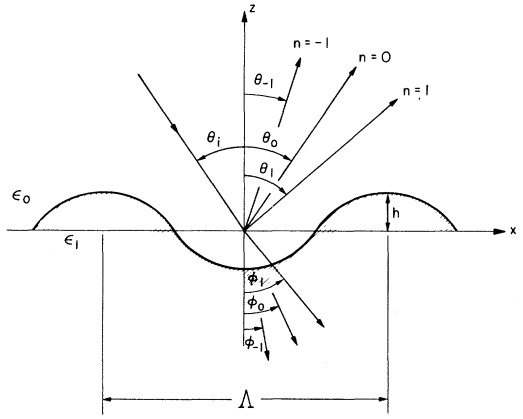

FIG. 5. Diffraction from a corrugated surface. The notation, explained in the text, is taken from Ref. 36.

ed in Ref. 36 in terms of the total fields and their normal derivatives at the surface. We have also assumed that $h/\lambda \ll 1$.

Henceforth we will be interested in the fields at the surface. We shall make use of Rayleigh's hypothesis, which consists of extending the outgoing wave solution down to the surface to match the boundary condition. Intuitively, this method is realistic in the limit where h/Λ is small, since for strong corrugation the contribution from evanescent fields, for example, is expected. Petit and Cadilhac[37] have shown that Rayleigh's hypothesis is strictly valid for $h/\Lambda < 0.072$, but it may be adequate for much larger ratios h/Λ.[38]

We now follow Ref. 36 again to express the surface fields in the form of

$$\hat{n}\cdot\vec{\nabla}\psi_1 = 2iK\sum_{n=-1}^{1}\beta_n^s e^{iK\alpha_n' x}, \tag{13a}$$

$$\psi_1 = 2\sum_{n=-1}^{1}\alpha_n^s e^{iK\alpha_n' x}. \tag{13b}$$

The new coefficients, α_n^s and β_n^s, have been calculated with the use of some results given in Ref. 36:

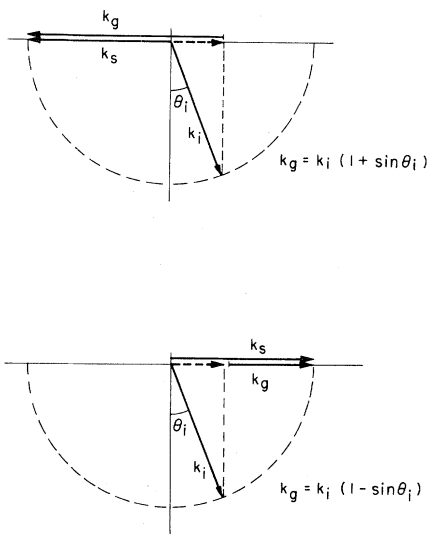

FIG. 6. $\vec{k}$-vector diagram for diffraction at grazing incidence, where $\vec{k}_i$ represents the incident wave, $\vec{k}_g$ the grating, and $\vec{k}_s$ the scattered wave. The figure shows the two possible grating spacings for angle of incidence θ_i.

$$\alpha_0^s = \frac{\beta_0^{1/2}}{\beta_0 + C_2'\beta_0'}, \tag{14a}$$

$$\alpha_{\pm1}^s = \frac{-i(hk/2)\alpha_0^s[-1+\alpha_0\alpha_{\pm1}-C_2'(K/k)(-1+\alpha_0'\alpha_{\pm1}'+\beta_0'\beta_{\pm1}')-C_2'\beta_{\pm1}\beta_0']}{\beta_{\pm1}+C_2'\beta_{\pm1}'}, \tag{14b}$$

$$\beta_0^s = -\beta_0'\alpha_0^s, \tag{14c}$$

$$\beta_{\pm1}^s = -\beta_{\pm1}'\alpha_{\pm1}^s - \frac{ihK}{2}\alpha_0^s(1-\beta_0'\beta_{\pm1}'-\alpha_0'\alpha_{\pm1}'), \tag{14d}$$

where $C_2' = k/K$ for a TM wave and $C_2' = K/k$ for a TE wave. In these expressions we have kept small quantities only to first order. We immediately note that the amplitude of the scattered waves at the surface, $\alpha_{\pm1}^s$ and $\beta_{\pm1}^s$, is proportional to the amplitude of the surface corrugation or ripple. This occurs because our calculation is exact to first order.

Finally, we calculate the normal component of the average Poynting vector $\mathscr{P}_n$ just inside the medium:

$$\mathscr{P}_n = (\vec{E}\times\vec{H}^*)_n + \text{c.c.}$$

$$\simeq P_0\left[1+P_c\cos\frac{2\pi}{\Lambda}x + P_s\sin\frac{2\pi}{\Lambda}x\right] \tag{15a}$$

$$= P_0\left[1+P_1\cos\left[\frac{2\pi}{\Lambda}x-\phi_p\right]\right], \tag{15b}$$

where

$$P_0 = \text{Re}\frac{\beta_0^s\alpha_0^{s*}}{K}, \tag{16}$$

$$P_c = \text{Re}\{C_2'[\beta_0^s(\alpha_1^s+\alpha_{-1}^s) + \alpha_0^{s*}(\beta_1^s+\beta_{-1}^s)]\}, \tag{17}$$

$$P_s = -\text{Im}\{C_2'[\beta_0^s(-\alpha_1^s+\alpha_{-1}^s) + \alpha_0^{s*}(\beta_1^s-\beta_{-1}^s)]\}, \tag{18}$$

$$P_1 = (P_c^2+P_s^2)^{1/2}, \tag{19}$$

$$\tan\phi_p = \frac{P_s}{P_c}. \tag{20}$$

These equations indicate that on the surface a spatially sinusoidal light-intensity distribution with spacing Λ exists, in addition to the dc or average

light intensity. This ac term comes from the interaction between waves of zero order and first order, and is proportional to the amplitude of the ripples through $\alpha^s_{\pm 1}$ or $\beta^s_{\pm 1}$. Obviously, the larger the amplitude of the ripples the stronger the ac spatial energy-flux term. We note that interactions between first-order waves are neglected since it is a second-order effect.

B. Dielectric function

By using Eqs. (14)–(20) we can compute the intensity or energy absorbed at any point at the surface, provided we know the dielectric function. We have used the Drude model for the permittivity of metals and semiconductors, since it is usually a good description for this type of solids at wavelengths in the infrared or in the visible. We obtain for the real and imaginary parts of ϵ in metals the following well-known expressions:

$$\epsilon_r = 1 - \frac{\omega_p^2}{\omega^2 + 1/\tau_c^2} , \tag{21a}$$

$$\epsilon_i = \frac{\omega_p^2}{\omega\tau_c(\omega^2 + 1/\tau_c^2)} , \tag{21b}$$

where ω is the laser frequency, ω_p is the plasma frequency, and τ_c is the relaxation time. For typical metals at room temperature $\hbar\omega_p$ is $\sim 10-20$ eV and $\tau_c \sim 10^{-14}$ s. Ujihara[39] has derived an analytical model for the evolution of ϵ with temperature. Walter[40] has recently criticized Ujihara's approach and suggested some adjustments. We shall, however, take a path similar to that of Ujihara, since it is essentially correct and since it provides an analytical expression for the permittivity as a function of temperature.

In the model the temperature dependence of ϵ comes from the variation of $\omega_c = 1/\tau_c$ (the electron-phonon collision frequency) through the temperature dependence of the phonon population. From the knowledge of the optical constants at one temperature ϵ_r and ϵ_i are known at all temperatures up to the melting point. Figure 7 shows the variation of the optical constants of aluminum from room temperature to melting point for two wavelengths of interest (ripples were reported only at 1.06 μm). The values for ω_p and τ_c at room temperature are those used by Ujihara. We note that there is some disagreement as to the exact values of these two quantities[39–41] in Al and other metals, but adoption of another pair of values will only slightly adjust the curve, which is obtained by eliminating τ_c between Eqs. (21a) and (21b):

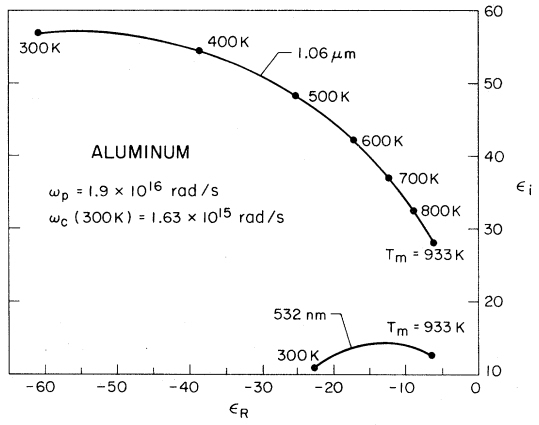

FIG. 7. Permittivity of aluminum as a function of temperature at two different wavelengths (from Ref. 39).

$$\left[\epsilon_r - 1 + \frac{\omega_p^2}{2\omega^2}\right]^2 + \epsilon_i^2 = \frac{\omega_p^4}{4\omega^4} . \tag{22}$$

We have also used the Drude model to describe the permittivity of semiconductors. We use a simplified lossy plasma model where the plasma frequency is now a function of the electron-hole density and $\omega\tau \gg 1$. In that case we write

$$\epsilon_r = \epsilon_\infty \left[1 - \frac{\omega_p^2}{\omega^2}\right] , \tag{23a}$$

$$\epsilon_i = \epsilon_\infty \frac{\omega_p^2}{\omega^3\tau_c} , \tag{23b}$$

and

$$\omega_p^2 = \frac{Ne^2}{m^*\epsilon_\infty} . \tag{24}$$

Here, e is the electronic charge, N is the carrier density, m^* is the reduced effective mass, ϵ_∞ is the dielectric constant of the empty solid at the frequency of interest, τ_c is the relaxation time, ω is the laser frequency, and ω_p is the plasma frequency. Under strong laser-light illumination the carrier concentration and the temperature may increase. The former effect is taken care of by the variation of the plasma frequency, while the latter effect should affect τ_c and ϵ_∞. If one wants to quantify the effect of temperature in general, problems occur: The temperature dependence of the different scattering mechanisms is not the same and, in general, the temperature variations of the optical constants of semiconductors are not very well known. Very recently, there has been a surge of interest in

the optical constants of semiconductors as a function of temperature. Silicon has been the main semiconductor investigated.[42–46] The variation of ϵ_r does not seem as spectacular as it is for metals, although ϵ_r is not constant in the whole solid phase; the variation of ϵ_i may be substantial, but in general $\epsilon_i \ll \epsilon_r$.

In Fig. 8 we show the influence of temperature on ϵ_r and ϵ_i. We have used the measurements of Jellison and Modine[46] for the absorption coefficient at 633 and 532 nm, and we have assumed that the temperature dependence of the real part of the refractive index measured at 633 nm by Murakami *et al.*[44] is not wavelength dependent and can be used at 532 nm as well.[47] The above-mentioned measurements are valid up to $\sim$1000 K, above which severe measurement problems appear.

Again, after elimination of ω_p between (23a) and (23b) one obtains

$$\epsilon_i = \frac{1}{\omega\tau_c}(\epsilon_\infty - \epsilon_r) . \tag{25}$$

Finally, we will also consider the case of liquid semiconductors, particularly liquid silicon, and also liquid metals. The properties of liquid metals are adequately represented by the Drude model.[48,49] Liquid silicon has similar properties to solid or liquid metals,[50,51] with large $|\epsilon_r|$ and ϵ_i. We shall use the results of Ref. 51.

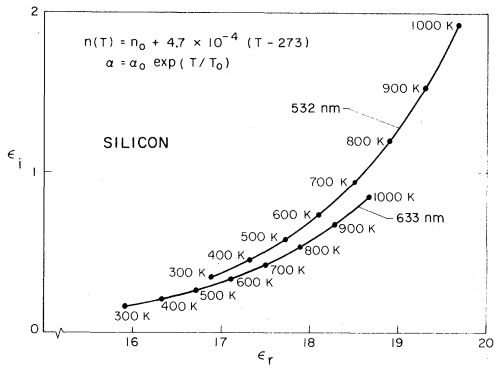

FIG. 8. Permittivity of silicon as a function of temperature at two different wavelengths (using data from Refs. 44 and 46). The curve stops at 1000 K, above which temperature no experimental data are available. At 532 nm, $\alpha = 5\times10^3$ cm^{-1} and $T_0 = 430$ K; at 633 nm, $\alpha = 2.1\times10^3$ cm^{-1} and $T_0 = 447$ K.

C. Nonuniform dielectric function

Consider a plane surface with periodic dielectric function. The permittivity of the medium can be expressed as

$$\epsilon_1' = \epsilon_1\left[1 + 2\delta e^{az}\cos\frac{2\pi}{\Lambda}x\right] , \tag{26}$$

where a stands for an attenuation coefficient in the $-z$ direction, Λ is the spatial period, and δ is a small quantity given by

$$\delta = \frac{\Delta\epsilon_r + i\Delta\epsilon_i}{2(\epsilon_r + i\epsilon_i)} . \tag{27}$$

Here, $\Delta\epsilon_r$ and $\Delta\epsilon_i$ represent the amplitude of the variation of the real and imaginary part of the dielectric function at the surface. Note that by using the Drude model we find

$$\Delta\epsilon_i = \frac{\Delta\epsilon_r}{\epsilon_i}\left[1 - \epsilon_r - \frac{\omega_p^2}{2\omega^2}\right] \tag{28a}$$

for a metal and

$$\Delta\epsilon_i = -\frac{1}{\omega\tau_c}\Delta\epsilon_r \tag{28b}$$

for a semiconductor.

We now consider the diffraction of a plane wave by such a periodic grating. The notation will be the same as in Sec. IVA, and we will show the results pertaining to a TM wave. From Maxwell's equations we find

$$\nabla^2\psi_1 + \omega^2\mu_0\epsilon_1'\psi_1 - \frac{1}{\epsilon_1'}\left[\frac{\partial\epsilon_1'}{\partial x}\frac{\partial\psi_1}{\partial x} + \frac{\partial\epsilon_1'}{\partial z}\frac{\partial\psi_1}{\partial z}\right] = 0 ,$$

which is rewritten as

$$\frac{\partial^2\psi_1}{\partial x^2} + \frac{\partial^2\psi_1}{\partial z^2} + K^2\left[1 + 2\delta e^{az}\cos\frac{2\pi}{\Lambda}x\right]\psi_1 + 2\delta e^{az}\left[\frac{2\pi}{\Lambda}\frac{\partial\psi_1}{\partial x}\sin\frac{2\pi}{\Lambda}x - a\frac{\partial\psi}{\partial z}\cos\frac{2\pi}{\Lambda}x\right] = 0 . \tag{29}$$

We let

$$\psi_1 = \sum_n B_n(z)e^{iK(\alpha_n' x - \beta_n' z)} . \tag{30}$$

We substitute ψ_1 into Eq. (29), keeping only terms with $n = 1$, 0, or -1, and use the slowly varying envelope approximation. We find

$$\frac{dB_0}{dz} = 0 , \tag{31a}$$

$$-2iK\beta'_1\frac{dB_1}{dz}+\delta K^2 e^{az}B_0 e^{-iK(\beta'_0-\beta'_1)z}\times\left[1+\frac{2\pi}{\Lambda}\frac{\alpha'_0}{K}+i\frac{\beta'_0 a}{K}\right]=0\,, \quad (31b)$$

$$-2iK\beta'_{-1}\frac{dB_{-1}}{dz}+\delta K^2 e^{az}B_0 e^{-iK(\beta'_0-\beta'_1)z}\times\left[1-\frac{2\pi}{\Lambda}\frac{\alpha'_0}{K}+i\frac{\beta'_0 a}{K}\right]=0\,. \quad (31c)$$

The magnetic field in the vacuum is still given by Eq. (11). The boundary conditions are

$$\frac{1}{\epsilon'_1}\frac{\partial\psi_1}{\partial z}\bigg|_{z=0}=\frac{1}{\epsilon_0}\frac{\partial\psi_0}{\partial z}\bigg|_{z=0}\,, \quad (32a)$$

$$\psi_1|_{z=0}=\psi_0|_{z=0}\,. \quad (32b)$$

By solving the system of differential equations [Eq. (31)], applying the boundary conditions [Eq. (32)], and keeping small quantities to first order only, we find

$$B_0=\frac{2\beta_0}{\beta_0+(k/K)\beta'_0}=2\alpha^s_0\,, \quad (33a)$$

$$B_{\pm1}=C_{\pm1}+C'_{\pm1}e^{\eta_{\pm1}z}=2\alpha^s_{\pm1}\,, \quad (33b)$$

where

$$\eta_{\pm1}=a-iK(\beta'_0-\beta'_{\pm1})\,, \quad (34a)$$

$$C'_{\pm1}=\frac{\delta B_0 K}{2i\beta'_{\pm1}\eta_{\pm1}}\left[1\pm\frac{2\pi}{\Lambda}\frac{\alpha'_0}{K}+i\frac{\beta'_0 a}{K}\right], \quad (34b)$$

$$C_{\pm1}=\frac{1}{\beta_{\pm1}+(k/K)\beta'_{\pm1}}\times\left\{-\left[\beta_{\pm1}+\frac{k}{K}\left[\beta'_{\pm1}+i\frac{\eta_{\pm1}}{K}\right]\right]\times C'_{\pm1}+\frac{k}{K}\delta\beta'_0 B_0\right\}, \quad (34c)$$

the tangential component of the electric field can be expressed in the form of

$$E_x(z=0)=\frac{1}{i\omega\epsilon'_1}\hat{n}\cdot\vec{\nabla}\psi_1=\frac{2K}{\omega\epsilon'_1}\sum_{n=-1}^{1}\beta^s_n e^{iK\alpha'_n x} \quad (35)$$

with

$$\beta^s_0=-\tfrac{1}{2}\beta'_0 B_0\,, \quad (36a)$$

$$\beta^s_{\pm1}=-\tfrac{1}{2}\left[C_{\pm1}\beta'_{\pm1}+C'_1\left[\beta'_{\pm1}+i\frac{\eta_{\pm1}}{K}\right]-2\delta\beta'_0\alpha^s_0\right]. \quad (36b)$$

V. RESULTS AND DISCUSSION

We are now ready to plot and discuss the results obtained in Sec. IV. We calculate the ac part of the absorbed power as a function of ripple spacing by using Eqs. (15)–(20). In Figs. 9–11, P_c is plotted versus the relative spatial period Λ/λ for a TM wave at normal incidence on a corrugated surface. We show the results for aluminum at melting point, crystalline silicon at different temperatures, and molten silicon. For copper we have obtained curves similar to those for aluminum and molten silicon. We have chosen a small ratio $h/\lambda=0.01$ (the rms surface roughness of the wafers and mirrors used in our experiments was a significant fraction of the wavelength). The variation of P_c in these figures is very abrupt around $\Lambda/\lambda=1$, with a sharp (negative) minimum at $\Lambda\approx\lambda$ and a broader (positive) maximum for $\Lambda\leq\lambda$. To decide which extremum corresponds to growth we remember that we are searching for a feedback mechanism in which the intensi-

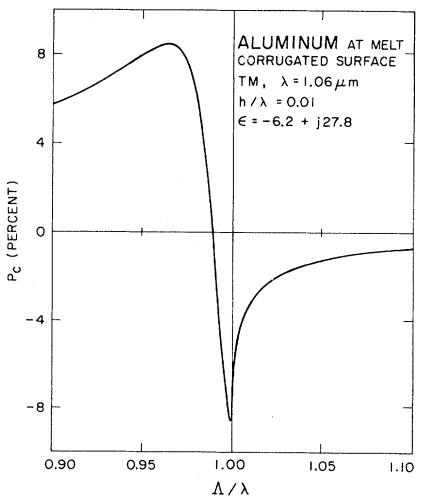

FIG. 9. P_c, the ac part of the absorbed power normalized to the "intrinsic" absorbed power, vs ripple spacing Λ normalized to the laser wavelength λ. The ratio of the surface corrugation height h to the wavelength λ is set to 1% and the normal incident wave is TM polarized. This graph is for aluminum at melting point and the permittivity is given by Fig. 7.

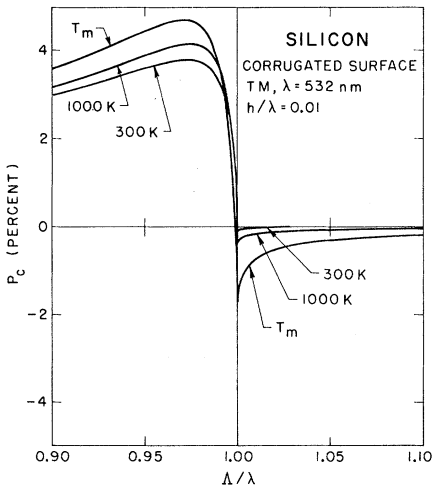

FIG. 10. P_c vs Λ/λ for solid silicon at 300 K, 1000 K, and melting point. The permittivity is given by Fig. 8 and its value at $T=T_M$ has been obtained by extrapolation.

ty pattern created by the initial disturbance reinforces the perturbation. We deduce from the geometry of Fig. 4 that $P_c<0$ corresponds to more energy being absorbed in the "hills" than in the "valleys," while $P_c>0$ corresponds to just the opposite situation. If thermal expansion is responsible for the ripples, then $P_c<0$ yields the desired positive feedback. If, however, the temperature dependence of the surface tension causes the ripples to grow, $P_c>0$ yields positive feedback. In that case more energy is indeed absorbed in the "valleys" where the temperature is thus highest, and the surface tension of the liquid lowest. The periodic variation of the surface tension pulls the liquid away from the valleys and positive feedback is established. Large-scale undulations induced by surface-tension gradients have been observed after cw laser treatment[52] but it is a very slow process not likely to play any significant role *during* illumination by very short laser pulses.[53]

In Figs. 12 and 13 we have plotted P_c vs Λ/λ for a TE wave in crystalline silicon at different temperatures and in molten silicon, respectively. It is apparent that the ac part of the absorbed power has a small maximum at $\Lambda=\lambda$ (compare the vertical scale with that in Figs. 9–11) and has an overall different shape. The impact of changing the angle of incidence is investigated in Figs. 14 and 15 for aluminum at melting temperature. From these figures we can understand the polarization dependence of the ripples. At normal incidence the ripple k vector will be parallel to the incident optical electric field (TM wave) since this corresponds to a much larger $|P_c|$. For oblique incidence the maximum ac terms occur very close to $\lambda/(1\pm\sin\theta)$. The amplitude of the two possible maxima is not equal, which probably explains why one spacing is often predominant.[17] Isenor,[10] Oron and Sorensen,[14] and Keilmann and Bai[19] have reported accurate measurements of Λ and have found that Λ is in fact slightly smaller than λ. The measurements of Ref. 14 are especially relevant, since they were made following irradiation of silicon at 1.06 μm. Oron and

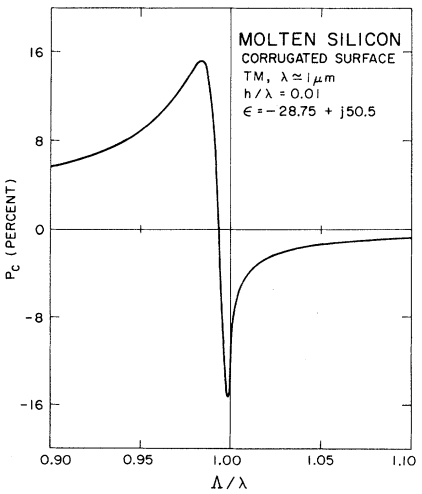

FIG. 11. P_c vs Λ/λ for molten silicon at melting point. The permittivity is obtained from Ref. 51.

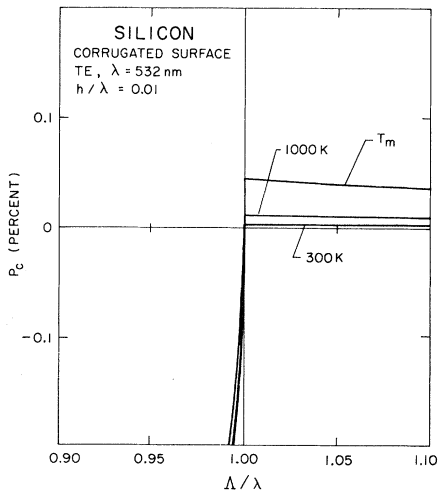

FIG. 12. P_c vs Λ/λ for solid silicon illuminated by TE polarized light. All the other parameters are those of Fig. 10.

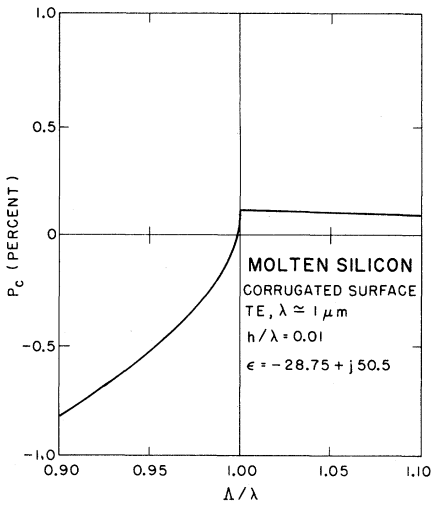

FIG. 13. P_c vs Λ/λ for molten silicon illuminated by TE polarized light. All the other parameters are those of Fig. 11.

Sorensen found a maximum (negative) departure of $<4\%$ from $\Lambda=\lambda/(1\pm\sin\theta)$, which is consistent in sign and amplitude with the results of our theory. We have found[21] similar small negative departures after illumination of copper at 1.06 μm.

We now turn our attention to the case of a periodic variation of permittivity. Figures 16—18 show some of our results for silicon and aluminum. Figures 6 and 7 illustrate that, as the temperature is increased, ϵ_r decreases in Al and Si (the sign of the variation also holds for Cu and GaAs), while the

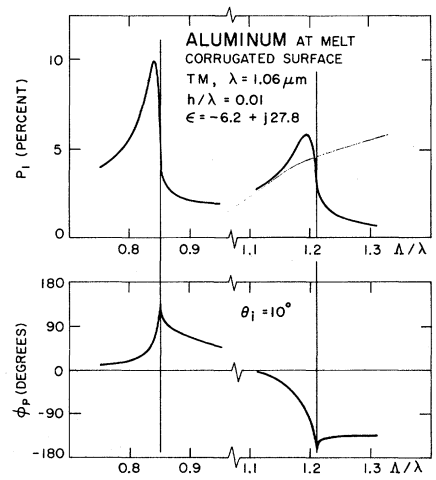

FIG. 14. Amplitude P_1 and phase ϕ_p of the normalized ac part of the absorbed power vs Λ/λ, for oblique incidence at $\theta_i=10°$. All other parameters are those of Fig. 9. The two vertical lines show the location of the spacings given by $\Lambda=\lambda/(1\pm\sin\theta_i)$.

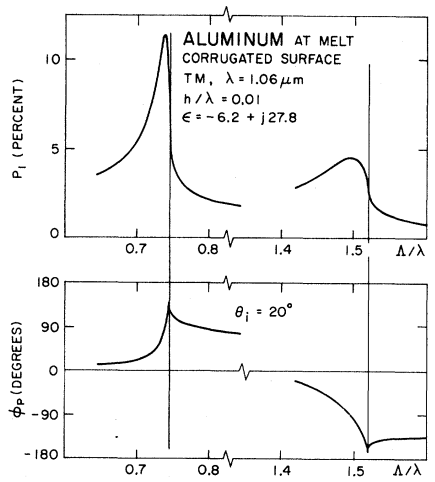

FIG. 15. P_1 and ϕ_p vs Λ/λ, for oblique incidence at $\theta_i=20°$.

variation of ϵ_i may be of any sign depending upon the material, its temperature, and the wavelength. For ϵ_r maximum at $x=0$ positive feedback is achieved for $P_c>0$. More power flows into the surface where ϵ_r is already larger (and the temperature is higher), and consequently ϵ_r increases faster. As shown in Fig. 17 this happens in solid silicon for $\Lambda/\lambda\approx1$, while the picture for molten silicon and the metals is quite different (Figs. 16 and 18). There is a broad minimum in P_c close to $\Lambda/\lambda=1$ and a very narrow local minimum at $\Lambda=\lambda$. De-

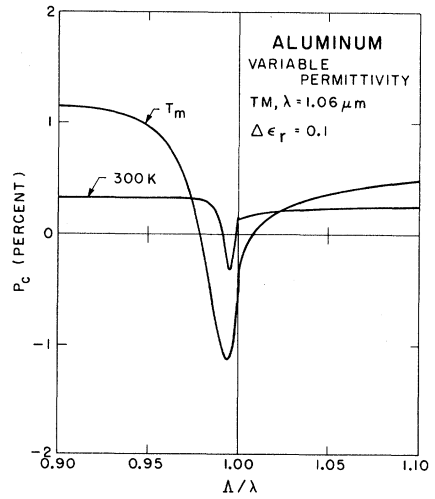

FIG. 16. P_c vs Λ/λ for aluminum at 300 K and melting point illuminated by a TM wave at 1.06 μm. The amplitude of the sinusoidal variation of the real part of the permittivity $\Delta\epsilon_r$ is 0.1 and that of the imaginary part is calculated by Eq. (28a) at the two different temperatures.

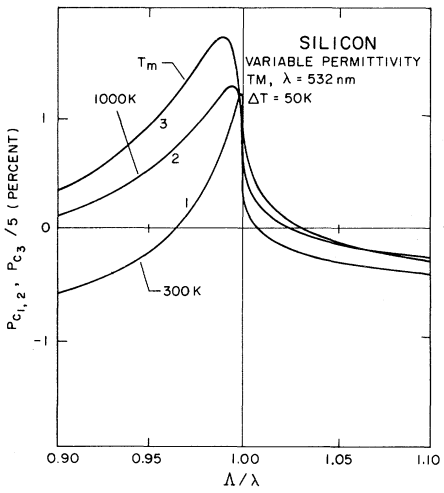

FIG. 17. P_c vs Λ/λ for solid silicon at 300 K, 1000 K, and melting point. The variation of permittivity corresponding to a sinusoidal temperature variation of 50 K is calculated from Fig. 8.

pending upon the choice of δ and the material, however, this local minimum can be reduced to an almost imperceptible kink in an otherwise smooth curve.

We have also investigated the effects of a variation of the dielectric function caused by fluctuations in the electron-hole plasma density. From Eqs. (32) and (24) it is clear that ϵ_r decreases and ϵ_i increases with increasing carrier density; ϵ_r may even become negative for $\omega_p > \omega$, but this requires an extremely dense plasma ($n \sim 10^{22}$ cm^{-3} for visible wavelength illumination). We have found for $\omega > \omega_p$ an extremum of P_c close to $\Lambda = \lambda$, but it does not fulfill the conditions for growth since the absorbed power turns out to be minimum where the electron-hole density is highest. Above the plasma frequency for $\omega < \omega_p$, not only is the feedback negative, but also the extremum of P_c is located far away from $\Lambda/\lambda = 1$, especially for the small negative real part of the dielectric function.

From these observations we conclude that a model in which the variation of the permittivity is predominant is not likely to allow for ripple growth. The corrugated surface model is much more likely to be adequate, since it provides for positive feedback. We note that the magnitude of the ac term of the absorbed power is the largest for metalliclike corrugated surfaces (compare the results for solid and liquid silicon). We have made an exhaustive search in the complex permittivity plane for regions of large potential growth (large negative P_c). The results are shown in Fig. 19. We indeed observe a significant difference between materials with positive and negative ϵ_r, with the latter displaying a larger growth coefficient. For small ϵ_i and negative ϵ_r, the ac part of the absorbed power is very large. This is to be expected: The "intrinsic" absorption decreases with ϵ_i, and therefore the ratio of the ripple-induced absorption to the intrinsic absorption increases.

The details of the feedback mechanism are beyond the scope of this paper. For example, it is clear that the permittivity of a corrugated surface under intense laser illumination will also vary

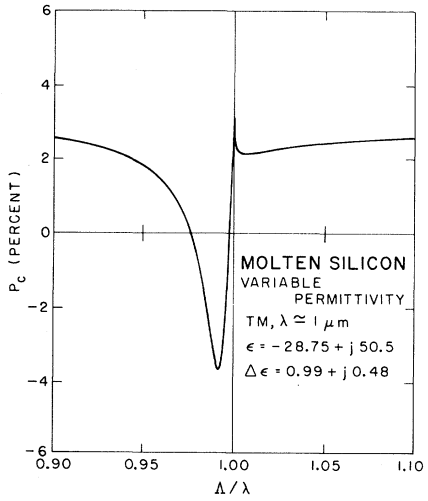

FIG. 18. P_c vs Λ/λ for molten silicon at melting point. The variation of the permittivity is calculated from Ref. 51.

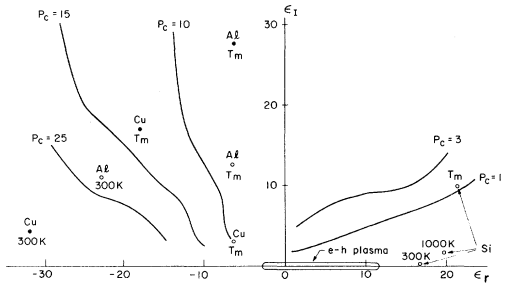

FIG. 19. Growth coefficient P_c in the complex permittivity plane for a corrugated surface ($h/\lambda = 0.01$) illuminated at normal incidence by a TM wave. P_c corresponds to the negative maximum in Figs. 9–11 and is expressed in percent. Open and closed circles represent the permittivity of materials at 532 nm and 1.06 μm, respectively. The point for Si at T_m is an extrapolation of the data of Fig. 8. The region representative of an electron-hole plasma corresponds to carrier density either below ($\epsilon_r > 0$) or above ($\epsilon_r < 0$) plasma resonance.

periodically under the action of differential heating. We have only considered one mechanism at a time, which is to say that one process is predominant. We have also speculated that for short pulses growth may occur in two distinct stages: When the laser pulse is on, growth begins as described in this paper; when the laser is turned off, growth may continue under the action of the varying stored energy.[52] However, this possible second stage is probably not significant. We have compared the conditions for ripple formation at 1.06 μm with two different laser pulse durations: 80 ns and 100 ps. At the adequate incident power level the ripples are always distinctly formed after illumination by a single 80-ns pulse; with a single picosecond pulse the ripples are usually faint, while repetitive illumination by several picosecond pulses usually results in well-established ripples.[21] This may indicate that while ~ 100 ps are sufficient for ripple formation, longer pulse illumination is preferable, since the time available for growth is much longer.[54]

It is also easy to explain why ripples can grow with illumination by increasing the number of laser shots, or propagate coherently after successive partially overlapping laser shots. In the first case the first shot induces minute ripple growth, too small to be visible under an electron or optical microscope[55]; the selection of one Fourier component according to Sec. III has not yet taken place; therefore, no organized surface structure is visible under scanning-electron or optical microscopy. As repetitive illumination is taking place the selection process slowly eliminates all the Fourier components except the one with the right spacing, which grows and finally becomes visible. Growth occurs from one shot to the next, and the incident power is much less than what is needed to create ripples under single-shot illumination.[17] In the second case the ripples in the first spot scatter the incident wave in the next spot and intensity fringes are produced with correct spacing; the ripples propagate coherently, the ripples in the first shot acting as a seed grating.

There are similarities between our problem and the anomalies encountered in metallic gratings,[56,57] which are known under the generic name of "Wood's anomaly." In both problems a possible source of surface excitation is a surface-plasmon polariton.[58] Light directly incident on a surface, such as in the experiments of interest here, will not generate these interface electromagnetic modes; however, if the surface is rough or corrugated, that possibility exists.[59–61] There are two reasons why we believe they are not the cause of the surface ripples. First, in semiconductors an extremely large number of carriers is required to satisfy $\omega_p > \omega$, a necessary condition for plasmons to occur. Then, the wave number $2\pi/\Lambda$ of the surface polariton is different from $2\pi/\lambda$, the difference increasing to infinity as

$$\omega_p \rightarrow \omega_p \mid_{\min} = \omega\sqrt{1+1/\epsilon_\infty} \ .$$

However, when $\omega_p \rightarrow \omega_p \mid_{\min}$ the surface polariton is tightly bound to the interface and the required electron-hole density is minimal. The surface polariton in the most favorable and likely situation has thus a wavelength quite different from λ. This is in contradiction with most experimental results, Keilmann and Bai[19] being the sole clear exception. In Ref. 19, however, the laser was tuned to overlap a reststrahlen vibrational region of quartz. Finally, we note that the presence of a periodic surface structure may alter that picture[59,60] by opening gaps in the (ω,k) dispersion curve at any multiple of the grating wave vector.

VI. CONCLUSION

We have developed a detailed theoretical model to account for the periodic surface structures observed during illumination of solids by intense laser pulses. In this model initial surface disturbances scatter part of the incident beam at almost grazing incidence; the interference of the scattered optical wave with the incident beam modulates the absorbed power in such a way that one Fourier component is reinforced and grows. We find the maximum positive feedback occurs when the spatial period $\Lambda \approx \lambda/(1 \pm \sin\theta)$, and the wave is TM polarized with respect to the grating formed by the ripples, in agreement with most experiments; the theory readily explains the coherent extension of ripples from one shot to another in a raster-scan mode, and the decreasing power density required for ripple formation in a repetitive shot-illumination experiment. The nature of the most likely initial perturbation is in height (even in polished samples the surface is far from ideally flat), and the growth coefficient (and to a smaller extent the actual spacing Λ) is dependent upon the actual value of the complex dielectric function. Our results indicate that growth will be much faster if the material is metalliclike, that is, for $\epsilon_r < 0$. This suggests that melting of the semiconductor is necessary.

Note added in proof. We wish for thoroughness to bring the attention of the reader to some additional recent results in the field of laser-induced surface ripples. Periodic surface structures have now been observed on insulators[62] and on silicon[63] using 10.6-μm lasers, as well as on metal films at short wavelengths.[64,65]

ACKNOWLEDGMENTS

We have enjoyed the interaction with many individuals, especially Dr. M. F. Becker, Dr. R. J. Nemanich, and Dr. F. Keilmann. We have appreciated receiving copies of unpublished work from R. J. Nemanich, F. Keilmann, H. M. van Driel, G. E. Jellison, Jr., and F. A. Modine. The assistance of J.-M. Heritier in computing has been most useful. Finally, this work was supported by the U.S. Air Force Office of Scientific Research.

---

*Permanent address: Shanxi University, Taiyuan, Shanxi, People's Republic of China.

[1]*Guide for Material Processing by Lasers,* edited by S. S. Charschan (Laser Institute of America, Baltimore, 1977).

[2]*Laser-Solid Interactions and Laser Processing—1978 (Materials Research Society, Boston),* Proceedings of the Symposium on Laser-Solid Interactions and Laser Processing, edited by S. D. Ferris, H. J. Leamy, and J. M. Poate (AIP, New York, 1979).

[3]*Laser and Electron-Beam Processing of Materials,* edited by C. W. White and P. S. Peercy (Academic, New York, 1980).

[4]*Laser and Electron-Beam Solid Interaction and Materials Processing,* edited by J. F. Gibbons, W. Hess, and T. Sigmon (Elsevier, New York, 1981).

[5]Special Issue on Laser Materials Interactions, IEEE J. Quantum Electron. 17 (1981).

[6]M. Siegrist, G. Kaech, and F. K. Kneubühl, Appl. Phys. 2, 45 (1973).

[7]D. C. Emmony, R. P. Howson, and L. J. Willis, Appl. Phys. Lett. 23, 598 (1973).

[8]C. T. Walters, Appl. Phys. Lett. 25, 696 (1974).

[9]L. J. Willis and D. C. Emmony, Opt. Laser Technol. 7, 222 (1975).

[10]N. R. Isenor, Appl. Phys. Lett. 31, 148 (1977).

[11]H. J. Leamy, G. A. Rozgonyi, T. T. Sheng, and G. K. Celler, Appl. Phys. Lett. 32, 535 (1978).

[12]G. N. Maracas, G. L. Harris, C. A. Lee, and R. A. McFarlane, Appl. Phys. Lett. 33, 453 (1978).

[13]G. A. Rozgonyi, H. J. Leamy, T. T. Sheng, and G. K. Celler, in *Laser-Solid Interactions and Laser Processing—1978 (Materials Research Society, Boston),* Proceedings of the Symposium on Laser-Solid Interactions and Laser Processing, edited by S. D. Ferris, H. J. Leamy, and J. M. Poate (AIP, New York, 1979), p. 457.

[14]M. Oron and G. Sorensen, Appl. Phys. Lett. 35, 782 (1979).

[15]R. M. Walser, M. F. Becker, J. G. Ambrose, and D. Y. Sheng, in *Laser and Electron-Beam Solid Interactions and Materials Processing,* edited by J. F. Gibbons, W. Hess, and T. Sigmon (Elsevier, New York, 1981), p. 177.

[16]A. K. Jain, V. N. Kulkarni, D. K. Sood, and J. S. Uppal, J. Appl. Phys. 52, 4882 (1981).

[17]P. M. Fauchet and A. E. Siegman, Appl. Phys. Lett. 40, 824 (1982).

[18]D. Haneman and R. J. Nemanich, Solid State Commun. 43, 203 (1982).

[19]F. Keilmann and Y. H. Bai, Appl. Phys. A29, 9 (1982).

[20]J. F. Young, J. E. Sipe, J. S. Preston, and H. M. van Driel, Appl. Phys. Lett. 41, 261 (1982).

[21]P. M. Fauchet and A. E. Siegman, CLEO Conference, Report No. WK6, Phoenix, 1982 (unpublished); P. M. Fauchet, Zhou Guosheng, and A. E. Siegman, IIIrd, Topical Meeting on Picosecond Phenomena, Garmisch-Partenkirchen, West Germany, 1982 (in press).

[22]C. Hill and D. J. Godfrey, J. Phys. (Paris), Colloq. 41, C4-79 (1980).

[23]K. Affolter, W. Luthy, and M. Wittmer, Appl. Phys. Lett. 36, 559 (1980).

[24]H. W. Lo and A. Compaan, Phys. Rev. Lett. 44, 1604 (1980).

[25]J. A. Van Vechten and M. Wautelet, Phys. Rev. B 23, 5543 (1981); M. Wautelet and J. A. Van Vechten, *ibid.* 23, 5551 (1981).

[26]J. A. Van Vechten and A. D. Compaan, Solid State Commun. 39, 867 (1981).

[27]R. F. Wood and G. E. Giles, Phys. Rev. B 24, 2923 (1981).

[28]B. Stritzker, A. Pospieszczyk, and J. A. Tagle, Phys. Rev. Lett. 47, 356 (1981).

[29]A. Lietoila and J. F. Gibbons, Appl. Phys. Lett. 40, 624 (1982).

[30]M. F. Becker, R. M. Walser, Y. K. Jhee, and D. Y. Sheng, Proc. Soc. Photo-Opt. Instrum. Eng. 322, 93 (1982).

[31]J. A. Van Vechten, Solid State Commun. 39, 1285 (1981).

[32]R. W. Rendell and K. L. Ngai, Bull. Am. Phys. Soc. 27, 235 (1982).

[33]For an elementary review, see H. J. Eichler, Opt. Acta

24, 631 (1977).
[34]V. I. Bespalov and V. I. Talanov, Zh. Eksp. Teor. Fiz. Pis'ma Red 3, 471 (1966) [JETP Lett. 3, 307 (1966)].
[35]A. J. Campillo, S. L. Shapiro, and B. R. Suydam, Appl. Phys. Lett. 23, 628 (1973).
[36]Shun-Lien Chuang and Jin Au Kong, Proc. IEEE 69, 1132 (1981).
[37]R. Petit and M. Cadilhac, C. R. Acad. Sci. Ser. B. 262, 468 (1966).
[38]A. Wirgin, Opt. Acta 27, 1671 (1980).
[39]K. Ujihara, J. Appl. Phys. 43, 2376 (1972).
[40]W. C. Walter, Proc. Soc. Photo-Opt. Instrum. Eng. 198, 109 (1979).
[41]M. Sparks and E. Loh, Jr., J. Opt. Soc. Am. 69, 847 (1979).
[42]H. A. Weakliem and D. Redfield, J. Appl. Phys. 50, 1491 (1979).
[43]M. O. Lampert, J. M. Koebel, and P. Siffert, J. Appl. Phys. 52, 4975 (1981).
[44]K. Murakami, K. Takita, and K. Masuda, Jpn. J. Appl. Phys. 20, L867 (1981).
[45]P. S. Peercy and W. R. Wampler, Appl. Phys. Lett. 40, 768 (1982).
[46]G. E. Jellison, Jr., and F. A. Modine Appl. Phys. Lett. 41, 180 (1982).
[47]This assumption is quite reasonable since, from a band-structure viewpoint, these two wavelengths are equivalent. Confirmation comes from Ref. 46, where it was shown that the temperature dependence of the absorption coefficient is almost wavelength independent for photon energies above the indirect gap and below the direct gap of silicon.
[48]N. R. Comins, Philos. Mag. 25, 817 (1972).
[49]T. E. Faber, *Introduction to the Theory of Liquid Metals,* Cambridge Monographs on Physics (Cambridge University Press, Cambridge, England, 1972).
[50]V. M. Glazov, S. N. Chizhevskaya, and N. N. Glagoleva, *Liquid Semiconductors* (Plenum, New York, 1969).
[51]K. M. Shvarev, B. A. Baum, and P. V. Gel'd, Fiz. Tverd. Tela. (Leningrad) 16, 3246 (1974) [Sov. Phys.—Solid State 16, 2111 (1975)].
[52]T. R. Anthony and H. E. Cline, J. Appl. Phys. 48, 3888 (1977).
[53]G. E. Possin, H. G. Perks, and S. W. Chiang, in *Laser and Electron-Beam Solid Interaction and Materials Processing,* edited by J. F. Gibbons, W. Hess, and T. Sigmon (Elsevier, New York, 1981), p. 73.
[54]As an interesting note, Dr. H. Kurz of Harvard University pointed out to us that, with the frequency-doubled 20-ps Nd:YAG system used in Professor N. Bloembergen's group, no ripple formation was seen (private communication). It is plausible that 20 ps is too short an illumination time for the growth process to occur.
[55]With our instruments, height variations as small as 20—50 Å cannot be seen.
[56]K. Outagawa, J. Opt. Soc. Am. 69, 333 (1979).
[57]*Electromagnetic Theory of Gratings,* Vol. 22 of *Topics in Current Physics,* edited by R. Petit (Springer, Berlin, 1980).
[58]E. Burstein, W. P. Chen, Y. J. Chen, and A. Harstein, J. Vac. Sci. Technol. 11, 1004 (1974).
[59]D. L. Mills, Phys. Rev. B 15, 3097 (1977).
[60]B. Laks, D. L. Mills, and A. A. Maradudin, Phys. Rev. B 23, 4965 (1981).
[61]J. M. Elson and C. C. Sung, Appl. Opt. 21, 1496 (1982).
[62]P. A. Temple and M. J. Soileau, IEEE J. Quantum Electron. 17, 2067 (1981).
[63]J. F. Figueira and S. J. Thomas, Appl. Phys. B28, 267 (1982).
[64]S. R. J. Brueck and D. J. Ehrlich, Phys. Rev. Lett. 48, 1678 (1982).
[65]R. M. Osgood and D. J. Ehrlich, Opt. Lett. 7, 385 (1982).

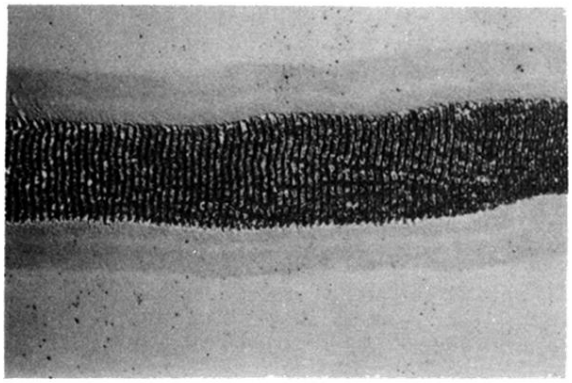

FIG. 1. Typical ripples obtained after raster scanning of GaAs at 1.06 μm. The angle of incidence is $\sim 37°$ and the spacing is ~ 2.5 μm.